

Deep Rational Reinforcement Learning

Quentin Delfosse¹Patrick Schramowski¹Martin Mundt¹Alejandro Molina¹Kristian Kersting¹²¹AI and Machine Learning Group, CS Department, TU Darmstadt, Germany²Centre for Cognitive Science, TU Darmstadt, Germany

Abstract

Latest insights from biology show that intelligence not only emerges from the connections between neurons but that individual neurons shoulder more computational responsibility than previously anticipated. This perspective should be critical in the context of constantly changing distinct reinforcement learning environments, yet current approaches still primarily employ static activation functions. In this work, we motivate why rationals are suitable for adaptable activation functions and why their inclusion into neural networks is crucial. Inspired by recurrence in residual networks, we derive a condition under which rational units are closed under residual connections and formulate a naturally regularised version: the recurrent-rational. We demonstrate that equipping popular algorithms with (recurrent-)rational activations leads to consistent improvements on Atari games, especially turning simple DQN into a solid approach, competitive to DDQN and Rainbow.

1 Introduction

Neural Networks' efficiency in approximating any function has made them the most used approximation function for many machine learning tasks. This is no different in reinforcement learning (RL), where the introduction of the DQN algorithm (Mnih et al., 2015) has sparked the development of various neural solutions. In concurrence with neuroscientific explanations of brainpower residing in combinations stemming

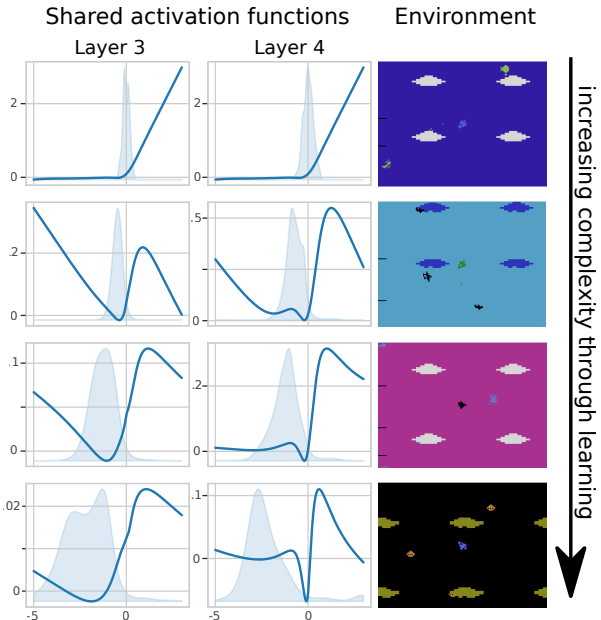


Figure 1: Neural plasticity due to trainable activation functions allows Deep RL to adapt to environments of increasing complexity. Rational activations (left columns), with shared parameters in the last two layers, evolve together with their input distributions when learning with DQN on Time Pilot. Each row corresponds to a state where a new, more challenging part of the environment (right column, e.g. increasing enemy speed and complexity) has been uncovered and is then additionally used for training.

from trillions of connections (Garlick, 2002), present advances have emphasised the role of the neural architecture (Liu et al., 2018; Xie et al., 2019). As such, improvements were obtained through a focus on enhancing algorithms through neural networks (Mnih et al., 2016; Haarnoja et al., 2018; Banerjee et al., 2021) and searching for well-performing architectural patterns (Cobbe et al., 2019; Miao et al., 2021).

However, research has also progressively shown that individual neurons shoulder more complexity than initially expected, and the latest results have demonstrated that dendritic compartments can compute complex functions (*e.g.* XOR), previously categorised as unsolvable by single-neuron systems (Gidon et al., 2020). This finding seems to have renewed interest in activation functions (Georgescu et al., 2020; Misra, 2020). In fact, many functions have been adopted across different domains (Redmon et al., 2016; Brown et al., 2020; Schulman et al., 2017). To reduce the bias introduced by a fixed activation function and achieve higher expressive power, one can further learn which activation function is performant for a particular task (Zoph & Le, 2017; Liu et al., 2018), learn to combine arbitrary families of activation functions (Manessi & Rozza, 2018), or find coefficients for polynomial activations as weights to be optimised (Goyal et al., 2019).

Whereas these prior approaches have all contributed to their respective investigated scenarios, there exists a finer approach that elegantly encapsulates the challenges brought on by reinforcement learning environments. Specifically, we can learn rational activation functions (Molina et al., 2020). Not only can rational activation functions converge to any continuous function, but they have further been proven to be better approximants than polynomials in terms of convergence (Telgarsky, 2017). Even more crucially, their ability to adapt while learning equips a model with high neural plasticity, *i.e.* capability to adjust to the environment and its transformations (Garlick, 2002). We argue that adapting to environmental changes is essential, making rational activation functions particularly suitable for dynamic RL environments. In contrast to task-specific and rigid activation functions, rational activations can thus adapt when environments drift and grow in complexity over time. To provide a visual intuition, we showcase an exemplary evolution of two rational activation functions together with the respective changing distribution of activations in the dynamic “Time Pilot” environment in Figure 1.

In this work, we therefore propose the use of plasticity via rational activations in deep neural RL approaches, as a central element to satisfy the requirements originating from diverse and dynamic environments. Apart from demonstrating their suitability, we further identify and address potential caveats to overcome remaining practical barriers. Our specific contributions are:

- (i) We show that neural plasticity is crucial for RL and that rational activations are adequate as adaptable activation functions.
- (ii) For this purpose, we highlight that rational activation functions do not only adapt their parame-

ters over time, but further prove that they can dynamically embed residual connections, which we refer to as residual plasticity.

- (iii) As introduction of additional representational capacity could lead to overfitting (Molina et al., 2020), we then introduce a recurrent-rational activation variant. By making use of weight-sharing across the rational activation function in different layers, we thus include necessary regularisation for RL (Farebrother et al., 2018; Roy et al., 2020; Yarats et al., 2021).
- (iv) We empirically demonstrate using *e.g.* Rainbow as baseline that inclusion of rational activations brings significant improvements on Atari games and that our introduced recurrence further increases performance.
- (v) Finally, we investigate the overestimation phenomenon of producing too large reward values, which has previously been argued to originate from an unsuitable representational capacity of the learning architecture (van Hasselt et al., 2016). As a result of our introduced neural and residual plasticity, such overestimation can practically be reduced.

We proceed as follows. We start off by arguing in favour of plasticity for deep reinforcement learning. Then we show how to realise using rational networks and present our empirical evaluation. Before concluding, we touch upon related work.

2 Plasticity via Rational Activation Functions for Deep RL

Let us start by arguing why deep reinforcement learning agents require extensive plasticity and showing that parametric rational activation functions,

$$R(x) = \frac{P(x)}{Q(x)} = \frac{\sum_{j=0}^m a_j x^j}{1 + \sum_{k=1}^n b_k x^k}, \quad (1)$$

where a_j and b_k are learnable parameters, provide this additional plasticity to the network.

2.1 Rational Neural Plasticity

As motivated in the introduction, RL is subject to inherent distribution shifts. During the training process agents progressively uncover new states (input drift) and, as the policy improves, the cumulative reward signal is modified (output drift). More precisely, for input drifts, we can distinguish environments according to how much they change through learning. For

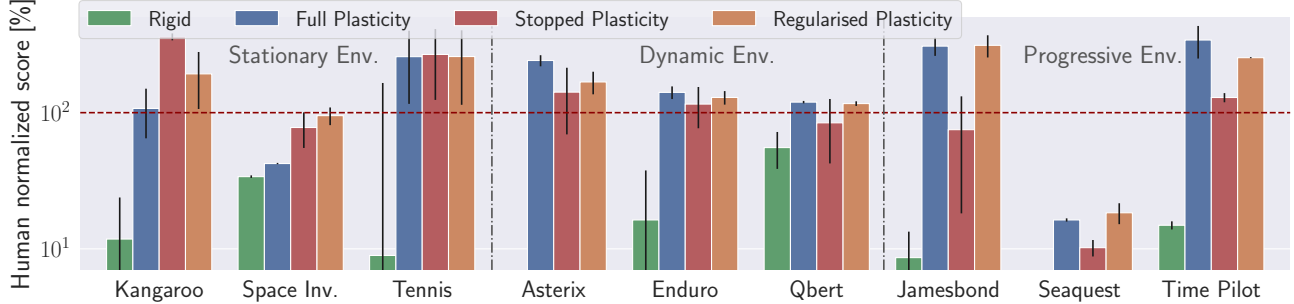


Figure 2: Neural plasticity is essential for reinforcement learning. Human normalised mean scores for rigid DQN agents, agents with full, “stopped” (tempered), and regularised plasticity are shown with standard deviation across 5 random seeded experimental repetitions. Larger scores are better. Stopped plasticity, allowing initial adaptation to the environments, but not their transformations in experimental repetitions, performs better on stationary environments. Regularised plasticity performs well across all environment types. Figure best viewed in colour. A full description of the environments and their types is provided in Appendix A.4.

simplicity, we categorise according to three intuitive categories: stationary, dynamic and progressive environments. To illustrate, consider the example of Atari 2600 games. Kangaroo, Space Invaders and Tennis can be characterised as stationary since the game’s input distribution does not change significantly. Asterix, Enduro and Qbert are dynamic environments, as different inputs are provided to the agents early in the game; hence no policy improvement is required to uncover (input) distribution shifts. On the contrary, Jamesbond, Seaquest, and Time Pilot are progressive environments. The agent needs to master early stages before being provided with additional states, *i.e.* exposed to a significant shift in the input distribution.

To deal with these distribution shifts, reinforcement learning environments need adaptive architectures with high neural plasticity. Such architectures have to adapt to their environment, but also to the changes of these environments during training. In Figure 2, we show how rational activation functions clearly provide RL networks with the necessary neural plasticity in the architecture. This aligns with the findings of Molina et al. (2020), who demonstrated the benefit of rational networks (RN) over fixed and other adaptive functions in supervised learning settings. The acquired plasticity seems to play an even more crucial role in RL. More precisely, by comparing agents with rigid networks (here a fixed Leaky ReLU baseline) to agents with full plasticity (*i.e.* agents with rational activation functions), we see that the flexibility of these functions boosts the agents to super-human performances on 7 out of 9 games. Especially in progressive environments, one can see the benefit of the neural plasticity provided by rational networks.

To highlight the requirement for plasticity even fur-

ther, we additionally distinguish between the plasticity of agents towards their specific environment and the plasticity allowing them to adapt while the environment itself is changing. To this end, we also show agents equipped with rational activations that are tempered in Figure 2. They have been extracted from agents with full plasticity, that adapted to their specific environment. Their plasticity is then “stopped” in repeated application to emphasise the necessity to continuously adapt during training. Whereas providing agents with such tempered, tailored to the task, activations already boost the performances, plasticity at all times is essential, particularly in the dynamic and above all progressive environments.

2.2 Rational Residual Plasticity

The prior paragraph has showcased the advantage of agents equipped with rational activation functions: their ability to update their parameters over time. However, we argue that the observed boost in performance is not only due to parameters adapting to distributional drifts. In addition to neural plasticity, rational activations embed one of the most popular techniques to stabilise training of deep neural networks; namely, they can dynamically make use of a residual connection. We refer to this as residual plasticity.

Veit et al. (2016) have exhibited the ability of residual networks to tackle the vanishing gradient problem. These networks were introduced following the intuition that it is easier to optimise the residual mapping than to optimise the original, unreferenced mapping (He et al., 2016). Formally, residual blocks of ResNets propagate an input \mathbf{X} through two paths: a transforming block of layers that preserves the dimensionality

(F) and a residual connection (identity). The output \mathbf{y} of such a block satisfies the following equation:

$$\mathbf{y}(\mathbf{X}) = F(\mathbf{X}) + \mathbf{X}. \quad (2)$$

Rationals are closed under residual connection and provide residual plasticity. Let us consider a rational function R of order (m, n) . We provide a proof in the Appendix (*cf.* Section A.1) that:

$$\mathbf{y}(\mathbf{X}) = R(\mathbf{X}) + \mathbf{X} = R'(\mathbf{X}), \quad (3)$$

with R' a rational function of order (m', n') , as long as $m' > n'$ is satisfied. In other words, rational activation functions of degree $m > n$ can embed residual connections if necessary. This property supports the experimental findings of Molina et al. (2020), who reported that using $m = n + 1$ provides the best empirical performance. Using the same degrees for numerator and denominator certifies asymptotic stability, but our derived configuration allows rationals to implicitly make use of residual connections. Importantly, note that these potential residual connections are not rigid, as these functions can progressively learn $a_j = 0$ for all $j > n$, *i.e.* we have residual plasticity.

To summarise, rational activation functions benefit from neural plasticity and benefit from similar advantages as residual blocks, such as avoiding potential vanishing gradients and easy convergence to the identity function if necessary.

Rationals as residual blocks. To also provide empirical evidence for the above described residual plasticity, we have investigated the practical extent to which specialised residual blocks, which have previously learned to approximate activation functions, can efficiently be replaced. Here, the intuition to exchange entire residual blocks is based on the previous findings of Greff et al. (2017). Specifically, the authors have observed that feature re-combinations do not occur inside the residual blocks but that transitions to new levels of representations occur during dimensionality changes. Residual blocks thus learn activation function-like behaviour, illustrating the crucial role of activation functions in learning strategies again. Therefore, we hypothesise that the aforementioned residual networks can draw more benefit from the residual plasticity of rational activations than from additional blocks. To test this hypothesis, we conduct lesioning experiments on a pretrained ResNet101 on the popular ImageNet (Deng et al., 2009) classification. We either remove complete residual blocks, corresponding to lesioning in (Veit et al., 2016), or replace them with rational activation functions that fulfil the residual connection condition derived above. The surrounding blocks and, in our case, the identity-initialised rational function are

	Recovery (%)	Lesioning	L2B3	L3B19	L3B22	L4B2
Training	Base [1]	100.9	90.5	100	58.9	
	Rat (ours)	101.1	104	120	91.1	
Testing	Base [1]	93.1	97.1	81.6	81.7	
	Rat (ours)	90.5	97.6	91.5	85.3	
	% dropped params	0.63	2.51	2.51	10.0	

Table 1: Rational functions improve lesioning. The recovery percentages for finetuned networks after lesioning (Veit et al., 2016)[1] of a ResNet layer’s (L) block (B) are shown. Residual blocks were lesioned, *i.e.* replaced with the identity (Base) or a rational (Rat) from a pretrained ResNet101 (44M parameters). Then, the surrounding blocks (and implanted rational activation function) are retrained for 15 epochs. Larger percentages are better, best results are in **bold**.

fine-tuned to recover from the block amputation. Our primary concern is thus to recover the modelling capabilities of the original architecture expressed through the training loss. The training and test accuracies for the lesioning experiments are shown in Table 1. We can clearly observe that rational activation functions lead to performance improvements that even surpass the original model (even when later introduced benefits of additional regularisation are not leveraged).

2.3 Natural Rational Regularisation

We have motivated and shown that the combination of neural and residual plasticity form the central pillars for why rational activation functions are desirable in deep RL. In particular, for dynamic and progressive environments, full plasticity has been observed to provide a substantial boost over rigid approaches in Figure 2. However, if we circle back to this figure and take a more careful look at the stationary environments, we can observe that our previously investigated tempered plasticity (for emphasis, initially allowed to tailor to the task but later “stopped” plasticity in experimental repetition) can also have an upper edge over full plasticity. Following the argument of the supervised experiments of Molina et al. (2020), this is because rational activation functions can also overfit in principle. In fact, overfitting in deep RL is a regularly encountered challenge, and prior works have highlighted the necessity for regularisation (Farebrother et al., 2018; Roy et al., 2020; Yarats et al., 2021).

To alleviate potential overfitting, we thus propose a naturally regularised version for rational activations. For this regularised variant, we again draw inspiration from residual blocks. In particular, Greff et al. (2017) have indicated that sharing the weights can improve learning performances, as shown in Highway (Lu &

Renals, 2016) and Residual (Liao & Poggio, 2016) Networks. In the spirit of these findings, we propose using recurrent-rational networks, which employ a novel type of regularisation, where the key idea is recurrence in the rational activation, by sharing the weights. As such, the input is propagated through different layers but always passed through the same rational activation function (with full plasticity). As one can see in Figure 2, agents equipped with such a regularised form of plasticity increase in performances on stationary environments and do not deteriorate performance in progressive environments.

3 Empirical Evidence for Plasticity

Our intention here is to investigate the benefits of neural plasticity through rational networks for deep reinforcement learning. That is, we investigated the following questions:

- (Q1) Do neural networks equipped with rational plasticity outperform rigid baselines?
- (Q2) Can neural plasticity make up for more heavy algorithmic RL advancements?
- (Q3) Can plasticity address the overestimation problem?

To this end, we compare¹ our rational networks and recurrent-rational networks using the original DQN architecture (Mnih et al., 2015) on 15 different games of the Atari 2600 domain (Brockman et al., 2017) and compare these architectures to ones equipped with the Leaky ReLU baseline as well as functions of the SiLU family (specifically introduced by for DQN on Atari environments by Elfwing et al. (2018)). We then compare increased neural plasticity provided by (recurrent-)rational networks to algorithm improvements, namely the Double DQN (DDQN) method (van Hasselt et al., 2016), that tackles DQN’s overestimation problem, as well as Rainbow (Hessel et al., 2018), that incorporates multiple algorithm improvements brought to DQN. Finally, we explain how neural plasticity can help readdress overestimation.

In practice, we used safe rational activation functions (Molina et al., 2020), i.e. we used the absolute value of the sum in the denominator to avoid poles. This stabilises training and makes the function continuous without creating instabilities. Rationals are shared across layers (thus adding only 10 parameters per layer). We base our experiments on the original neural networks used by the DQN, DDQN and SiLU authors

and the same hyper-parameters (*cf.* Section A.6.2 in Appendix) across all the Atari agents. For a fair comparison, we report performances using the normalised (*cf.* Appendix A.6) mean and standard deviation of the scores obtained by fully trained agents over five seeded reruns for every (D)DQN agent. However, since often only the best performing RL agent (among the reruns) is reported in the literature, we also provide a table of max scores in the Appendix. For Rainbow, unfortunately, we can only report the results of single runs. A single run already took more than 40 days on a NVIDIA Tesla V100 GPU; rainbow is known to be computationally quite demanding (Obando-Ceron & Castro, 2021).

(Q1) DQN with neural plasticity is better than rigid baselines. To start off, we compared RL agents with rational plasticity to rigid DQN baselines: Leaky ReLU, as well as agents equipped with SiLU activation function ($\text{SiLU}(x) = x \cdot \text{sigmoid}(x)$) and its derivative dSiLU inside the DQN networks. Elfwing et al. (2018) showed that using SiLU or a combination of SiLU (on convolutional layers) and its derivative dSiLU (on fully connected layers) in DQN, agents perform better on several games than ReLU networks. SiLU (and dSiLU) are—to our knowledge—the only activation functions specifically designed for RL applications.

The results are summarised in Table 2. As one can see, DQN with (regularised) plasticity clearly outperforms the rigid activation counterparts. Furthermore, RL agents with functions of the SiLU family outperform Leaky ReLU ones on less than half of the games. More importantly, they do not perform better than non-rigid rational networks, as only on one game out of 15 (Kangaroo), agents equipped with SiLU are better than DQN with full plasticity. In stark contrast, DQN with both plasticity types always outperformed Leaky ReLU baselines. DQN with regularised plasticity even obtains higher mean scores than the non-regularised versions 9 out of 15 times. Actually, both DQN with neural plasticity (with and without regularisation) obtained super-human performances on 11 out of 15 games.

This clearly shows that rational plasticity pays off for (deep) reinforcement learning agents, providing an affirmative answer to question (Q1).

(Q2) DQN with neural plasticity can beat more complex RL approaches such as Rainbow. To investigate this, we considered the Rainbow algorithm (Hessel et al., 2018). Rainbow aggregates multiple improvements brought to the DQN—Double Q-learning, prioritised experience replay, duelling network architecture, multi-step target, distributional learning and stochastic networks—and is widely used also as base-

¹30.000 GPU hours, carried out on a DGX-2 Machine with Nvidia Tesla V100 with 32GB.

Algorithm		DQN		DDQN		DQN with Plasticity	
Network Type	LReLU	SiLU	d+SiLU	LReLU	full	regularised	
Asterix	1.85 \pm 1.2	0.52 \pm 0.6	2.14 \pm 1.4	48.9 \pm 17.7	242 \pm 23.5	168 \pm 32.6•	
Battlezone	11.4 \pm 7.0	21.2 \pm 15.0	11.3 \pm 6.7	68.2 \pm 34.8	70.1 \pm 2.1•	77.4 \pm 8.7	
Breakout	558 \pm 166	93.9 \pm 57.6	11.7 \pm 14.0	286 \pm 122	1134 \pm 130•	1210 \pm 36.0	
Enduro	16.3 \pm 21.3	37.0 \pm 17.7	0.37 \pm 0.5	47.7 \pm 18.1	141 \pm 15.0	129 \pm 14.7•	
Jamesbond	8.62 \pm 6.4	6.08 \pm 3.7	5.28 \pm 4.4	10.7 \pm 11.1	308 \pm 48.5•	312 \pm 59.5	
Kangaroo	11.8 \pm 12.5	128 \pm 95.6•	13.9 \pm 18.5	17.2 \pm 14.5	107 \pm 43.1	193 \pm 86.8	
Pong	101 \pm 5.5	96.1 \pm 12.0	104 \pm 3.3	91.3 \pm 30.8	107.0 \pm 2.4•	107.3 \pm 2.7	
Qbert	55.4 \pm 17.1	14.2 \pm 17.0	2.74 \pm 0.2	74.0 \pm 21.7	120 \pm 2.8	117 \pm 4.9•	
Seaquest	0.57 \pm 0.4	3.67 \pm 4.1	0.18 \pm 0.2	2.17 \pm 0.9	16.3 \pm 0.5•	18.4 \pm 3.3	
Skiing	-90.7 \pm 37.9	-111 \pm 0.7	-85.5 \pm 43.4	-86.9 \pm 46.6	-59.5 \pm 60.7	-60.2 \pm 56.1•	
Spaceinvaders	33.9 \pm 4.3	33.1 \pm 11.9	32.4 \pm 12.4	31.0 \pm 1.0	42.3 \pm 3.1•	95.1 \pm 17.7	
Tennis	8.94 \pm 17.3	26.3 \pm 53.3	78.5 \pm 64.3	32.1 \pm 51.6	257.8 \pm 2.8•	258.3 \pm 5.2	
Timepilot	14.9 \pm 14.3	19.3 \pm 31.0	18.3 \pm 38.1	6.61 \pm 7.5	341 \pm 105	253 \pm 11.0•	
Tutankham	0.03 \pm 2.8	58.2 \pm 48.6	2.89 \pm 4.0	24.4 \pm 0.4	130 \pm 10.7•	134 \pm 29.3	
Videopinball	440 \pm 123	55.8 \pm 61.9	-4.03 \pm 32.5	626 \pm 241	1616 \pm 1026	906 \pm 539•	
# Wins	0/15	0/15	0/15	0/15	6/15	9/15	
# Super-Human	3/15	1/15	1/15	2/15	11/15	11/15	

Table 2: Neural plasticity leads to vast performance improvements. Normalised mean scores and standard deviations (in percentage, *cf.* Appendix A.6 for the equation) of rigid baselines (*i.e.* DQN and DDQN with Leaky ReLU, DQN with SiLU and SiLU + dSiLU), as well as DQN with full plasticity and regularised plasticity, are reported over five experimental random seeded repetitions (larger mean values are better). The best results are highlighted in **bold** and runner-ups denoted with • markers. The last rows summarise the number of times best mean scores were obtained by each agent and the number of super-human performances.

line (Lin et al., 2020; Hafner et al., 2021).

Figure 3 shows the learning curves of Rainbow and DQN, both with Leaky ReLU baselines, as well as with full and regularised plasticity. While Rainbow is computationally much heavier (\sim 8 times slower than DQN in our experiments, with higher memory needs), its rigid form never outperforms the much simpler and more efficient DQN with neural plasticity, and its rational versions dominate in only 1 out of 8 games (Enduro). Rainbow even lost to vanilla DQN on 3 games.

Therefore, DQN agents with plasticity are competitive alternatives to the complicated and expensive Rainbow method, answering question **(Q2)** affirmatively.

Neural plasticity directly tackles the overestimation problem. Revisiting Figure 3, one can see that Rainbow variants are worst on dynamic environments such as Jamesbond, Time Pilot and particularly Seaquest. On these games, the performance of rigid (Leaky ReLU) DQN progressively decreases.

Such drops are well known in the literature and typically attributed to the overestimation problem of DQN. This overestimation is due to the combination of bootstrapping, off-policy learning and a function ap-

proximator (neural network) operating by DQN. van Hasselt et al. (2016) show that inadequate flexibility of the function approximator (either insufficient or excessive) can lead to a slight overestimation of a state-action pair. The max operator in the update rule of DQN then propagates this overestimation while learning with the replay buffer. The overestimated states can stay in the buffer long before the agent revisits (and thus update) them. This can lead to catastrophic performance drops. To mitigate this problem, van Hasselt et al. (2016) introduced a second network to separate action selection from action evaluation, resulting in Double DQN (DDQN).

We compared the original DDQN approach (*i.e.* equipped with Leaky ReLU), which is rigid, to vanilla DQN with neural plasticity on Atari games. As one can see in Table 2, DQN with plasticity outperforms even the more complex DDQN approach on every considered Atari game. This reinforces the affirmative answer to **(Q1)** from earlier on.

More important, we computed the relative overestimation values of the (D)DQN, both with and without

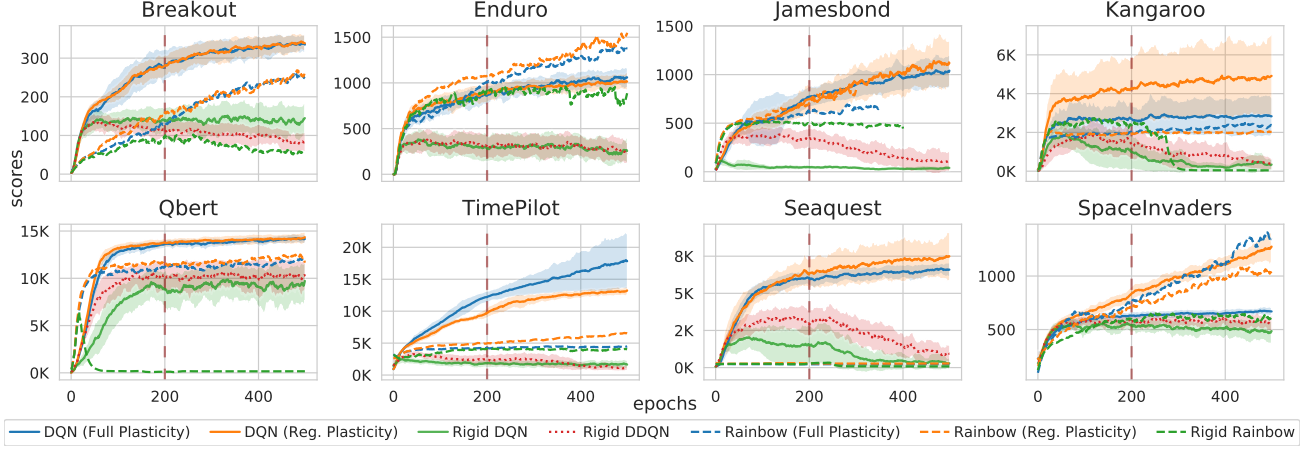


Figure 3: Networks with neural plasticity compared to rigid baselines (DQN, DDQN and Rainbow) over five random seeded runs on eight Atari 2600 games. The resulting mean scores (lines) and standard deviation (transparent area) during training are shown. As one can see, DDQN does not resolve performance drops but only delays them (e.g. particularly pronounced on Seaquest). A figure including the evolution of every agent on all Atari 2600 games is provided in Appendix A.3. Best viewed in colour.

neural plasticity, following:

$$\text{overestimation} = \frac{\text{Q-value} - R}{R}, \quad (4)$$

where the return R corresponds to $R = \sum_{t=0}^{\infty} \gamma^t r_t$, with the observed reward r_t and the discount factor γ .

The results are summarised in Figure 4. As one can see, plasticity helps to reduce overestimation drastically. The game for which DDQN substantially reduces the overestimation are Jamesbond, Kangaroo, Tennis, Time Pilot and Seaquest. For these games, DDQN obtains the best performances among all rigid variants only on Jamesbond (*cf.* Table 2). Moreover, Figure 3 shows that the performance drops of corresponding DDQN rigid agents are only delayed and not prevented. The performance drops thus happen after the 200th epoch, after which the training of RL agents is usually stopped.

While we agree that overestimation might play a role in the performance drops on progressive environments (*cf.* Figure 3: Jamesbond, TimePilot and Seaquest), it cannot fully explain the phenomena. Instead, RL agents with higher neural plasticity can handle these games much better while not having considerably more parameters. Hence, we advocate that neural plasticity better deals with distribution shifts due to the dynamics of games with progressive environments.

Surprisingly, (regularised) neural plasticity not only works well on challenging progressive environments but also on much simpler ones such as Enduro, Pong

and Qbert, where more flexibility is likely to hurt. Luckily, overestimation due to high flexibility does not happen here, as one can see in Figure 4. Moreover, the activation functions learned for these games have a simpler profile than those learned on more complicated games like Kangaroo and Time Pilot. Details are provided in Appendix A.5. The rational activation functions thus seem to adapt to the environment’s complexity and the policy they need to model. This clearly provides an affirmative answer to (Q3).

All experimental results together clearly show that neural plasticity through rational networks considerably benefits deep reinforcement learning.

4 Related Work

Next to the related work discussed throughout the paper, our work on plasticity is also related to research lines on neural architecture search and activation functions in deep reinforcement learning.

Neural Architectures for Deep Reinforcement Learning. Cobbe et al. (2019) showed that the architecture of IMPALA (Espeholt et al., 2018), notably containing residual blocks, improved the performances over the original Nature-CNN (Mnih et al., 2015) one. Motivated by these findings, Miao et al. (2021) recently applied neural architecture search to reinforcement learning tasks and demonstrated that the optimal architecture and its complexity highly depends on the environment. Their search provides different

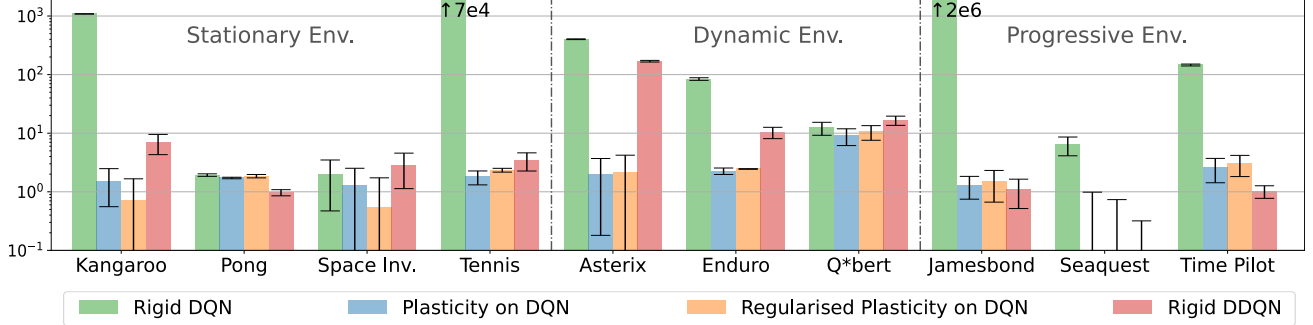


Figure 4: Plasticity naturally reduces overestimation. Relative overestimation values (log scale, smaller values are better, see Eq. 4) of both rigid DQN and DDQN, as well as DQN with full and regularised plasticity. Each trained agent is evaluated on 100 completed games (5 random seeds per game per agent, *i.e.* 20 completed games for each seed). Agents with additional plasticity lower overestimation values as much or further than rigid DDQN ones, which has originally been introduced explicitly to this end. Figure best viewed in colour.

architectures for different environments, with varying activation functions across layers and potential residual connections. Continuously modifying the complexity of the neural network based on the noisy reward signal in a complex architectural space is extremely resource demanding, particularly for large scale problems. Many RL specific problems, such as noisy rewards (Henderson et al., 2018), input interdependency (Mnih et al., 2015), policy instabilities (Haarnoja et al., 2018), sparse rewards, difficult credit assignment (Mesnard et al., 2021), complicate an automated architecture search.

The choice of activation functions. Many different activation functions have been adopted across different domains (*e.g.* Leaky ReLU in YOLO (Redmon et al., 2016), Tanh in PPO (Schulman et al., 2017), GELU in GPT-3 (Brown et al., 2020)), indicating that the relationship between the choice of activation functions and performance of neural networks is highly dependent on the task, architecture, hyper-parameters and the dataset (or environment). As shown in this paper, parametric functions provide plasticity. (Molina et al., 2020) showed that rationals outperform other learnable activation function types. Telgarsky showed that rationals are locally better approximants than polynomials. Finally, Boullé et al. (2020) later showed that composing low-degree rational functions require fewer parameters to approximate a ReLU Network. While this is indeed more efficient in terms of parameters, compositions of rationals functions need to be computed sequentially, which is slower when using gradient descent methods.

5 Limitations and Future Work

We have shown the benefits of rational activation functions for deep RL as a consequence of both their neural and residual plasticity. In our derivation for closure under residuals, we have deduced that the degree of the polynomial in the numerator needs to be greater than that of the denominator. Correspondingly, we have based our empirical investigations on the degrees (5, 4). Interesting future work would be to further automatically select suitable degrees that fulfil this condition. As additional future avenues, one should also explore neural plasticity in more advanced deep RL approaches, including short term memory (Kapturowski et al., 2019), finer exploration strategy (Badia et al., 2020), or include neural plasticity into architecture search, without having to perform a combinatorial search across possible activation functions.

6 Societal Impact Statement

The noisy optimisation performed in our deep RL experiments are particularly costly and therefore contribute to carbon emissions. However, this is usually a means to an end, as reinforcement algorithms are also used to optimise energy distribution and consumption in several applications. The plasticity entailed by rational activation functions provides significant performance improvement with negligible difference in memory cost and compute time. That said, deep (RL) methods are well-known for their potential miss-use in society, but notably, our proposition should not further add onto existing unfortunate aspects and miss-use scenarios.

7 Conclusions

It is well known from biology that neural plasticity allows our brains to adapt and change, i.e., learn new things. Here we showed how to achieve an end-to-end differentiable form of plasticity for deep reinforcement learning using rational activation functions, a class of trainable activation recently introduced.

Actually, inspired by recurrence in residual networks, we derived a condition under which rational units are closed under residual connections and formulated a naturally regularised version: the recurrent-rational networks, showing that they provide a regularised plasticity, beneficial for deep reinforcement learning. Our experimental evaluation demonstrates that equipping popular RL algorithms with neural plasticity results in consistent improvements on Atari games, turning effortless, simple DQN into a strong baseline, being competitive to DDQN and Rainbow.

References

Adrià Puigdomènech Badia, Pablo Sprechmann, Alex Vitvitskyi, Zhaohan Daniel Guo, Bilal Piot, Steven Kapturowski, Olivier Tielemans, Martín Arjovsky, Alexander Pritzel, Andrew Bolt, and Charles Blundell. Never give up: Learning directed exploration strategies. In *8th International Conference on Learning Representations (ICLR)*, 2020.

Chayan Banerjee, Zhiyong Chen, and Nasimul Noman. Improved soft actor-critic: Mixing prioritized off-policy samples with on-policy experience. *CoRR*, abs/2109.11767, 2021.

Nicolas Boullé, Yuji Nakatsukasa, and Alex Townsend. Rational neural networks. In Hugo Larochelle, Marc'Aurelio Ranzato, Raia Hadsell, Maria-Florina Balcan, and Hsuan-Tien Lin (eds.), *Advances in Neural Information Processing Systems 33: Annual Conference on Neural Information Processing Systems (NeurIPS)*, 2020.

Greg Brockman, Vicki Cheung, Ludwig Pettersson, Jonas Schneider, John Schulman, Jie Tang, and Wojciech Zaremba. Openai gym. *CoRR*, abs/1707.06347, 2017.

Tom B. Brown, Benjamin Mann, Nick Ryder, Melanie Subbiah, Jared Kaplan, Prafulla Dhariwal, Arvind Neelakantan, Pranav Shyam, Girish Sastry, Amanda Askell, Sandhini Agarwal, Ariel Herbert-Voss, Gretchen Krueger, Tom Henighan, Rewon Child, Aditya Ramesh, Daniel M. Ziegler, Jeffrey Wu, Clemens Winter, Christopher Hesse, Mark Chen, Eric Sigler, Mateusz Litwin, Scott Gray, Benjamin Chess, Jack Clark, Christopher Berner, Sam McCandlish, Alec Radford, Ilya Sutskever, and Dario Amodei. Language models are few-shot learners. In Hugo Larochelle, Marc'Aurelio Ranzato, Raia Hadsell, Maria-Florina Balcan, and Hsuan-Tien Lin (eds.), *Advances in Neural Information Processing Systems 33: Annual Conference on Neural Information Processing Systems (NeurIPS)*, 2020.

Karl Cobbe, Oleg Klimov, Christopher Hesse, Taehoon Kim, and John Schulman. Quantifying generalization in reinforcement learning. In *Proceedings of the 36th International Conference on Machine Learning, (ICML)*, 2019.

Jia Deng, Wei Dong, Richard Socher, Li-Jia Li, Kai Li, and Li Fei-Fei. Imagenet: A large-scale hierarchical image database. In *IEEE Computer Society Conference on Computer Vision and Pattern Recognition (CVPR)*, 2009.

Carlo D'Eramo, Davide Tateo, Andrea Bonarini, Marcello Restelli, and Jan Peters. Mushroomrl: Simplifying reinforcement learning research. *CoRR*, abs/2001.01102, 2020.

Stefan Elfwing, Eiji Uchibe, and Kenji Doya. Sigmoid-weighted linear units for neural network function approximation in reinforcement learning. *Neural Networks*, 2018.

Lasse Espeholt, Hubert Soyer, Rémi Munos, Karen Simonyan, Volodymyr Mnih, Tom Ward, Yotam Doron, Vlad Firoiu, Tim Harley, Iain Dunning, Shane Legg, and Koray Kavukcuoglu. IMPALA: scalable distributed deep-rl with importance weighted actor-learner architectures. In Jennifer G. Dy and Andreas Krause (eds.), *Proceedings of the 35th International Conference on Machine Learning (ICML)*, 2018.

Jesse Farnbrother, Marlos C. Machado, and Michael Bowling. Generalization and regularization in DQN. *CoRR*, abs/1810.00123, 2018.

D Garlick. Understanding the nature of the general factor of intelligence: the role of individual differences in neural plasticity as an explanatory mechanism. *Psychological review*, 2002.

Mariana-Iuliana Georgescu, Radu Tudor Ionescu, Nicolae-Catalin Ristea, and Nicu Sebe. Non-linear neurons with human-like apical dendrite activations. *CoRR*, abs/2003.03229, 2020.

Albert Gidon, Timothy Adam Zolnik, Pawel Fidzinski, Felix Bolduan, Athanasia Papoutsis, Panayiota Poirazi, Martin Holtkamp, Imre Vida, and Matthew Evan Larkum. Dendritic action potentials and computation in human layer 2/3 cortical neurons. *Science*, 2020.

Mohit Goyal, Rajan Goyal, and Brejesh Lall. Learning activation functions: A new paradigm of understanding neural networks. *CoRR*, abs/1906.09529, 2019.

Klaus Greff, Rupesh Kumar Srivastava, and Jürgen Schmidhuber. Highway and residual networks learn unrolled iterative estimation. In *5th International Conference on Learning Representations (ICLR)*, 2017.

Tuomas Haarnoja, Aurick Zhou, Pieter Abbeel, and Sergey Levine. Soft actor-critic: Off-policy maximum entropy deep reinforcement learning with a stochastic actor. In Jennifer G. Dy and Andreas Krause (eds.), *Proceedings of the 35th International Conference on Machine Learning (ICML)*, 2018.

Danijar Hafner, Timothy P. Lillicrap, Mohammad Norouzi, and Jimmy Ba. Mastering atari with discrete world models. In *9th International Conference on Learning Representations (ICLR)*, 2021.

Kaiming He, Xiangyu Zhang, Shaoqing Ren, and Jian Sun. Deep residual learning for image recognition. In *2016 IEEE Conference on Computer Vision and Pattern Recognition (CVPR)*, 2016.

Peter Henderson, Riashat Islam, Philip Bachman, Joelle Pineau, Doina Precup, and David Meger. Deep reinforcement learning that matters. In Sheila A. McIlraith and Kilian Q. Weinberger (eds.), *Proceedings of the Thirty-Second Conference on Artificial Intelligence AAAI*, 2018.

Matteo Hessel, Joseph Modayil, Hado van Hasselt, Tom Schaul, Georg Ostrovski, Will Dabney, Dan Horgan, Bilal Piot, Mohammad Gheshlaghi Azar, and David Silver. Rainbow: Combining improvements in deep reinforcement learning. In Sheila A. McIlraith and Kilian Q. Weinberger (eds.), *Proceedings of the Thirty-Second Conference on Artificial Intelligence (AAAI)*, 2018.

Steven Kapturowski, Georg Ostrovski, John Quan, Rémi Munos, and Will Dabney. Recurrent experience replay in distributed reinforcement learning. In *7th International Conference on Learning Representations (ICLR)*, 2019.

Qianli Liao and Tomaso A. Poggio. Bridging the gaps between residual learning, recurrent neural networks and visual cortex. *CoRR*, abs/1604.03640, 2016.

Zhixuan Lin, Yi-Fu Wu, Skand Vishwanath Peri, Weihao Sun, Gautam Singh, Fei Deng, Jindong Jiang, and Sungjin Ahn. SPACE: unsupervised object-oriented scene representation via spatial attention and decomposition. In *8th International Conference on Learning Representations (ICLR)*, 2020.

Chenxi Liu, Barret Zoph, Maxim Neumann, Jonathon Shlens, Wei Hua, Li-Jia Li, Li Fei-Fei, Alan L. Yuille, Jonathan Huang, and Kevin Murphy. Progressive neural architecture search. In Vittorio Ferrari, Martial Hebert, Cristian Sminchisescu, and Yair Weiss (eds.), *15th European Conference on Computer Vision (ECCV)*, 2018.

Liang Lu and Steve Renals. Small-footprint deep neural networks with highway connections for speech recognition. In Nelson Morgan (ed.), *17th Annual Conference of the International Speech Communication Association (INTERSPEECH)*, 2016.

Franco Manessi and Alessandro Rozza. Learning combinations of activation functions. In *24th International Conference on Pattern Recognition (ICPR)*, 2018.

Thomas Mesnard, Theophane Weber, Fabio Viola, Shantanu Thakoor, Alaa Saade, Anna Harutyunyan, Will Dabney, Thomas S. Stepleton, Nicolas Heess, Arthur Guez, Eric Moulines, Marcus Hutter, Lars Buesing, and Rémi Munos. Counterfactual credit assignment in model-free reinforcement learning. In Marina Meila and Tong Zhang (eds.), *Proceedings of the 38th International Conference on Machine Learning (ICML)*, 2021.

Yingjie Miao, Xingyou Song, Daiyi Peng, Summer Yue, Eugene Brevdo, and Aleksandra Faust. RL-DARTS: differentiable architecture search for reinforcement learning. *CoRR*, abs/2106.02229, 2021.

Diganta Misra. Mish: A self regularized non-monotonic activation function. In *31st British Machine Vision Conference 2020, (BMVC)*, 2020.

Volodymyr Mnih, Koray Kavukcuoglu, David Silver, Andrei A. Rusu, Joel Veness, Marc G. Bellemare, Alex Graves, Martin A. Riedmiller, Andreas Fidjeland, Georg Ostrovski, Stig Petersen, Charles Beattie, Amir Sadik, Ioannis Antonoglou, Helen King, Dharshan Kumaran, Daan Wierstra, Shane Legg, and Demis Hassabis. Human-level control through deep reinforcement learning. *Nature*, 2015.

Volodymyr Mnih, Adrià Puigdomènech Badia, Mehdi Mirza, Alex Graves, Timothy P. Lillicrap, Tim Harley, David Silver, and Koray Kavukcuoglu. Asynchronous methods for deep reinforcement learning. In Maria-Florina Balcan and Kilian Q. Weinberger (eds.), *Proceedings of the 33rd International Conference on Machine Learning (ICML)*, 2016.

Alejandro Molina, Patrick Schramowski, and Kristian Kersting. Padé activation units: End-to-end learning of flexible activation functions in deep networks. In *8th International Conference on Learning Representations (ICLR)*, 2020.

Johan S. Obando-Ceron and Pablo Samuel Castro. Revisiting rainbow: Promoting more insightful and inclusive deep reinforcement learning research. In *Proceedings of the 38th International Conference on Machine Learning (ICML)*, 2021.

Joseph Redmon, Santosh Kumar Divvala, Ross B. Girshick, and Ali Farhadi. You only look once: Unified, real-time object detection. In *IEEE Conference on Computer Vision and Pattern Recognition (CVPR)*, 2016.

Julien Roy, Paul Barde, Félix G. Harvey, Derek Nowrouzezahrai, and Chris Pal. Promoting coordination through policy regularization in multi-agent deep reinforcement learning. In Hugo Larochelle, Marc'Aurelio Ranzato, Raia Hadsell, Maria-Florina Balcan, and Hsuan-Tien Lin (eds.), *Advances in Neural Information Processing Systems 33: Annual Conference on Neural Information Processing Systems 2020 (NeurIPS)*, 2020.

John Schulman, Filip Wolski, Prafulla Dhariwal, Alec Radford, and Oleg Klimov. Proximal policy optimization algorithms. *CoRR*, abs/1707.06347, 2017.

Matus Telgarsky. Neural networks and rational functions. In Doina Precup and Yee Whye Teh (eds.), *Proceedings of the 34th International Conference on Machine Learning (ICML)*, Proceedings of Machine Learning Research, 2017.

Hado van Hasselt, Arthur Guez, and David Silver. Deep reinforcement learning with double q-learning. In Dale Schuurmans and Michael P. Wellman (eds.), *Proceedings of the Thirtieth Conference on Artificial Intelligence (AAAI)*, 2016.

Andreas Veit, Michael J. Wilber, and Serge J. Belongie. Residual networks behave like ensembles of relatively shallow networks. In Daniel D. Lee, Masashi Sugiyama, Ulrike von Luxburg, Isabelle Guyon, and Roman Garnett (eds.), *Advances in Neural Information Processing Systems 29: Annual Conference on Neural Information Processing Systems (NeurIPS)*, 2016.

Sirui Xie, Hehui Zheng, Chunxiao Liu, and Liang Lin. SNAS: stochastic neural architecture search. In *7th International Conference on Learning Representations (ICLR)*, 2019.

Changqing Xu, Mingyue Wang, and Xian Li. Generalized vandermonde tensors. *Frontiers of Mathematics in China*, 2016.

Denis Yarats, Ilya Kostrikov, and Rob Fergus. Image augmentation is all you need: Regularizing deep reinforcement learning from pixels. In *9th International Conference on Learning Representations, (ICLR)*, 2021.

Barret Zoph and Quoc V. Le. Neural architecture search with reinforcement learning. In *5th International Conference on Learning Representations (ICLR)*, 2017.

A Appendix

As mentioned in the main body, the appendix contains additional materials and supporting information for the following aspects: the proof of residual connection embedded in rational activation functions (A.1), every final and maximal scores obtained by the reinforcement learning agents used in our experiments (A.2), the evolutions of these scores (A.3), the different environment types with illustrations of their changes (A.4), graphs of the learned rational activation functions (A.5) and technical details for reproducibility (A.6).

A.1 Proof of the residual connection of rational functions

In the main body, we explained that rational activation functions whose order respect $m < n$ embed residual connections. In this section, we provide a proof to support this claim: we show that rational functions that respect the aforementioned condition are closed under residual connection.

Let us consider a rational function $R = P/Q$ of order (m, n) , with coefficients $A^{[m]} = (a_j)_{j=0}^m \in \mathbb{R}^{m+1}$ of P and $B^{[n]} = (b_i)_{i=0}^n \in \mathbb{R}^{n+1}$ of Q (with $b_0 = 1$).

We denote by \otimes (resp. \oslash) the Hadamard product (resp. division). For a given tensor $\mathbf{X} \in \mathbb{R}^{n_1 \times \dots \times n_x}$, corresponding to the input of the rational function at the end of a arbitrary layer of a given neural network.

We derive $\mathbf{X}^{\otimes k} = \bigotimes_{i=1}^k \mathbf{X}$. Furthermore, we use $GV^{[k]}(\mathbf{X}) = [\mathbf{1}, \mathbf{X}, \mathbf{X}^{\otimes 2}, \dots, \mathbf{X}^{\otimes k}] \in \mathbb{R}^{(n_1 \times \dots \times n_x) \times k+1}$ to denote the tensor containing the powers up to k of the tensor \mathbf{X} . Note that $GV^{[k]}$ can be understood as a generalised Vandermonde tensor, similar as introduced in (Xu et al., 2016).

For $V^{[k]} = (v_i)_{i=0}^k \in \mathbb{R}^{k+1}$, we express by $GV^{[k]}.V^{[k]} = \sum_{i=0}^k v_i \mathbf{X}^{\otimes i}$ the weighted sum over the tensor elements in the last dimension.

Now, we apply the rational activation function R with residual connection elementwise to \mathbf{X} :

$$\begin{aligned} \mathbf{y}(\mathbf{X}) &= R(\mathbf{X}) + \mathbf{X} = GV^{[m]}(\mathbf{X}).A^{[m]} \oslash GV^{[n]}(\mathbf{X}).B^{[n]} + \mathbf{X} \\ &= (GV^{[m]}(\mathbf{X}).A^{[m]} + \mathbf{X} \otimes GV^{[n]}(\mathbf{X}).B^{[n]}) \oslash GV^{[n]}(\mathbf{X}).B^{[n]} \\ &= (GV^{[m]}(\mathbf{X}).A^{[m]} + GV^{[n+1]}(\mathbf{X}).B_0^{[n+1]}) \oslash GV^{[n]}(\mathbf{X}).B^{[n]} \\ &= GV^{[\max(m, n+1)]}(\mathbf{X}).C^{[\max(m, n+1)]} \oslash GV^{[n]}(\mathbf{X}).B^{[n]} = R'(\mathbf{X}), \end{aligned}$$

where $B_0^{[n+1]} = (b_{0,i})_{i=0}^{n+1} \in \mathbb{R}^{n+2}$ (with $b_{0,0} = 0$ and $b_{0,i} = b_{i-1}$ for $i \in \{1, \dots, n+1\}$) and $C^{[\max(m, n+1)]} = (c_j)_{j=0}^{\max(m, n+1)}$ with $c_j = a_j + b_{j-1}$, $a_j = 0$ for all $j \notin \{0, \dots, m\}$ and $b_j = 0$ for all $j \notin \{0, \dots, n\}$.

This proves that such rational activation functions (of order $m > n$) are able to embed residual connections if necessary.

A.2 Complete raw scores table for Deep Reinforcement Learning

Through this work, we showed the performance superiority of reinforcement learning agents that embed additional plasticity provided by learnable rational activation functions. We used human normalised scores (*cf.* Eq. 6) for readability. For completeness, we provide in this section final raw scores of every trained agent. As many papers provide the maximum obtained score among every epochs and every agents, even if we consider it to be an inaccurate and noisy indicator of the agents performances, for which random actions can still be taken (because of ϵ -greedy strategy also being used in evaluation). A fairer indicator to compare methods is the mean score. We thus also provide final mean scores (of agents retrained among 5 seeded reruns) with standard deviation. We start off by providing the human scores used for normalisation (provided by van Hasselt et al. (2016), in Table 5), then provide final mean and maximum obtained raw scores of every agent.

Human scores used for normalisation:

Asterix: 7536, Battlezone: 33030, Breakout: 27.9, Enduro: 740.2, Jamesbond: 368.5, Kangaroo: 2739, Pong: 15.5, Q*bert: 12085, Seaquest: 40425.8, Skiing: -3686.6, Space Invaders: 1464.9, Tennis: -6.7, Time Pilot: 5650, Tutankham: 138.3, Video Pinball: 15641.1

Final mean scores of other agents:

Algorithm	Random	DQN			DDQN	DQN with Plasticity	
Network type	-	LReLU	SiLU	d+SiLU	LReLU	full	regularised
Asterix	67.9 \pm 2.2	206 \pm 90	107 \pm 45	228 \pm 108	3723 \pm 1324	18109\pm1755	12621 \pm 2436
Battlezone	788 \pm 38	4464 \pm 2291	7612 \pm 4877	4429 \pm 2183	22775 \pm 11265	23403 \pm 701	25749\pm2837
Breakout	0.14 \pm 01	155 \pm 46	26.2 \pm 16	3.4 \pm 3.89	79.4 \pm 33.8	315 \pm 36	336\pm10
Enduro	0 \pm 0	121 \pm 158	274 \pm 131	2.77 \pm 3.41	353 \pm 134	1043\pm111	957 \pm 109
Jamesbond	6.39 \pm 0.41	37.6 \pm 23.6	28.4 \pm 13.8	25.5 \pm 16.2	45.2 \pm 40.7	1122 \pm 176	1137\pm216
Kangaroo	14.2 \pm 0.9	335 \pm 342	3500 \pm 2607	393 \pm 504	484 \pm 395	2940 \pm 1175	5266\pm2365
Pong	-20.2 \pm 0	15.9 \pm 2	14.1 \pm 4.3	16.9 \pm 1.2	12.4 \pm 11	18 \pm 0.9	18.1\pm1
Q*bert	40.6 \pm 2.8	6715 \pm 2058	1754 \pm 2048	371 \pm 28	8954 \pm 2616	14436\pm336	14080 \pm 593
Seaquest	20.1 \pm 0.4	250 \pm 162	1504 \pm 1677	94.6 \pm 87.2	898 \pm 353	6603 \pm 200	7461\pm1321
Skiing	-16104 \pm 92	-27365 \pm 4794	-29890 \pm 4	-26725 \pm 5485	-26892 \pm 5881	-23487\pm7624	-23582 \pm 7058
Space Inv.	51.6 \pm 1.1	531 \pm 62	520 \pm 169	509 \pm 176	490 \pm 15	650 \pm 45	1395\pm251
Tennis	-23.9 \pm 0.0	-22.4 \pm 3.0	-19.4 \pm 9.2	-10.4 \pm 11.1	-18.4 \pm 8.9	20.5 \pm 0.5	20.6\pm0.9
TimePilot	688 \pm 30	1428 \pm 739	1644 \pm 1566	1594 \pm 1918	1016 \pm 401	17632\pm5242	13261 \pm 576
Tutankham	3.51 \pm 0.54	3.55 \pm 4.3	81.9 \pm 66	7.41 \pm 5.96	36.4 \pm 0	179 \pm 15	184\pm40
VideoPinb.	6795 \pm 461	45683 \pm 11383	11730 \pm 5941	6439 \pm 3336	62151 \pm 21791	149712\pm91219	86942 \pm 48143

Table 3: Final mean raw scores (with std. dev.) of rigid baselines (*i.e.* DQN and DDQN with Leaky ReLU, DQN with SiLU and SiLU + dSiLU), as well as DQN with full plasticity (*i.e.* using rational activation functions) and regularised plasticity (*i.e.* using recurrent-rational ones) on Atari 2600 games, averaged over 5 seeded reruns (larger mean values are better).

Maximum obtained scores:

Algorithm	Random	DQN			DDQN	DQN with Plasticity	
Network type	-	LReLU	SiLU	d+SiLU	LReLU	full	regularised
Asterix	71	9250	3400	3800	20150	84950	49700
Battlezone	843	88000	81000	70000	97000	78000	94000
Breakout	0	427	370	344	411	864	864
Enduro	0	1243	928	1041	1067	1946	1927
Jamesbond	6	5600	5750	700	7500	9250	13300
Kangaroo	15	14800	15600	10200	13000	16200	16800
Pong	-20	21	21	21	21	21	21
Q*bert	45	19425	11700	5625	19200	24325	25075
Seaquest	20	7440	8300	740	15830	9100	26990
Skiing	-15997	-5987	-6505	-6267	-5359	-5368	-5612
Space Inv.	53	2435	2205	2460	2290	2490	3790
Tennis	-23	8	1	-1	4	24	36
Time Pilot	730	11900	15500	12500	12200	72000	28000
Tutankham	4	249	267	267	274	334	309
VideoPinb.	7599	998535	950250	338512	991669	997952	998324

Table 4: Maximum obtained scores (with std. dev.) of rigid baselines (*i.e.* DQN and DDQN with Leaky ReLU, DQN with SiLU and SiLU + dSiLU), as well as DQN with full plasticity (*i.e.* using rational activation functions) and regularised plasticity (*i.e.* using recurrent-rational ones) on Atari 2600 games, averaged over 5 seeded reruns (larger values are better).

Final mean and maximum obtained scores of Rainbow agents:

Evaluation	Final Mean Scores			Max. Obtained Scores		
	Plasticity	rigid	full	regularised	rigid	full
Breakout	52	279	303	383	569	569
Enduro	844	1473	1470	1388	1973	1964
Kangaroo	40	2157	2139	6300	6000	4800
Q*bert	149	11931	11551	16125	23550	23550
Seaquest	82	247	282	920	1280	1280
Space Inv.	595	1263	1157	2070	3395	2875
Time Pilot	3926	5386	6411	12700	15900	15900

Table 5: Final mean and maximum obtained scores obtained by rigid Rainbow agents (*i.e.* using Leaky ReLU), as well as Rainbow with full (*i.e.* using rational activation functions) and regularised (*i.e.* using recurrent-rational ones) plasticity (only 1 run because of computational cost, larger values are better).

A.3 Evolution of the scores on every game

The main part present some graphs that compares performance evolutions of the Rainbow and DQN agents with plasticity, as well as Rigid DQN, DDQN and Rainbow agents. We provide hereafter the evolution of the scores of every tested DQN and the DDQN agents on the complete game set. DQN agents with higher plasticity are always the best-performing ones. Experiments on several games (e.g. Jamesbond, Seaquest) show that using DDQN does not prevent the agent's performance drop but only delays it.

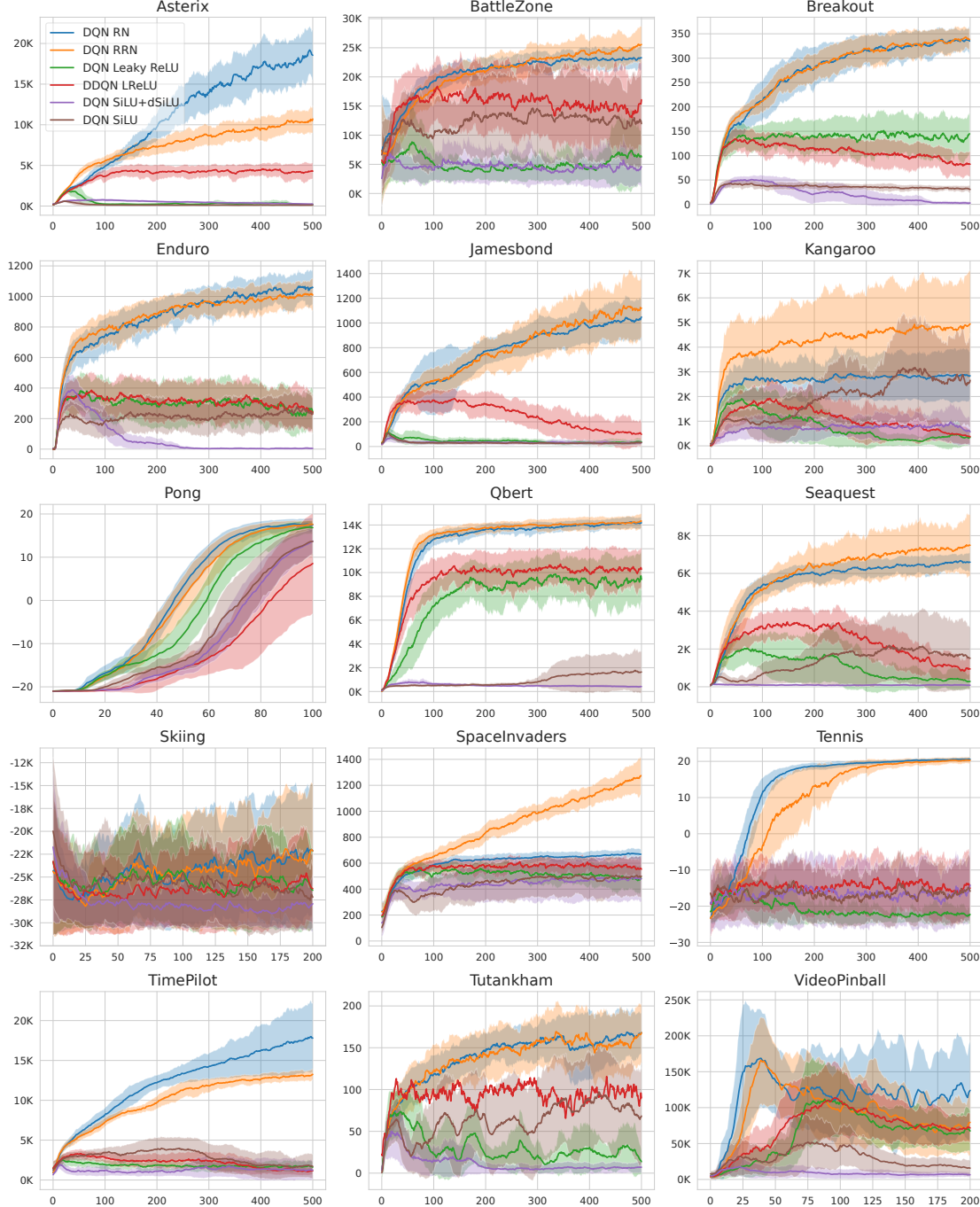


Figure 5: Smoothed (*cf.* Eq. 7) evolutions of the scores on every tested game for DQN agents with full (*i.e.* using rational activation functions) and regularised (*i.e.* using recurrent-rational ones) plasticity, and original DQN agents using Leaky ReLU, SiLU and SiLU+dSiLU, as well as for DDQN agents with Leaky ReLU.

A.4 Environments types: stationary, dynamics and progressive

The used environments have been separated in 3 categories, describing their potential changes through agents learning. This categorisation is here illustrated with frames of the tested games. As one can see: Breakout, Kangaroo, Pong, Skiing, Space Invaders, Tennis, Tutankham and VideoPinball can be categorised as **stationary environment**, as changes are minimal for the agents in these games. Asterix, BattleZone, Q*bert and Enduro present environment changes, that are early reached by the playing agents, and are thus **dynamic environments**. Finally, Jamesbond, Seaquest and Time Pilot correspond to **progressive environments**, as the agents needs to master early changes to access new parts of these environments.

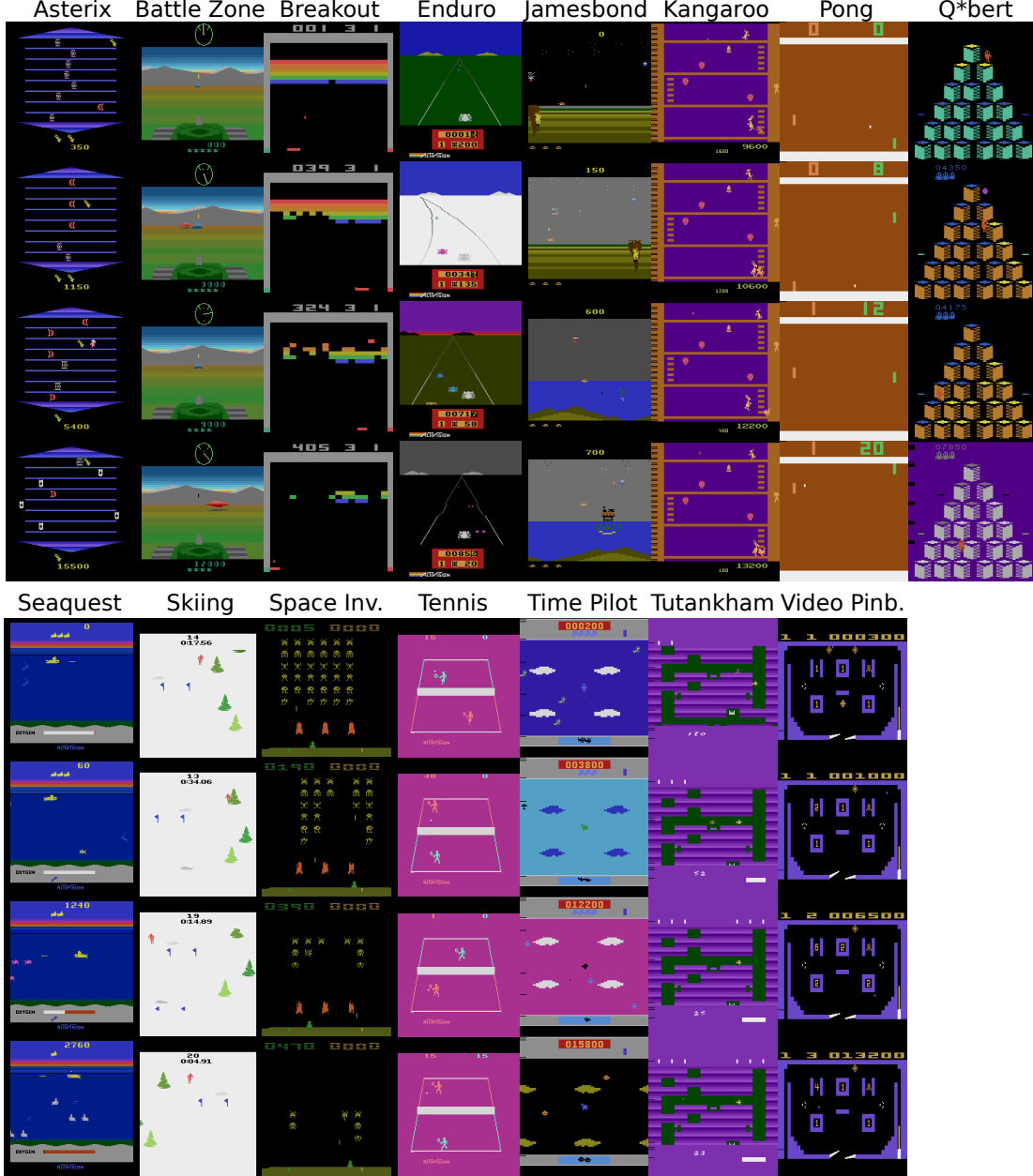
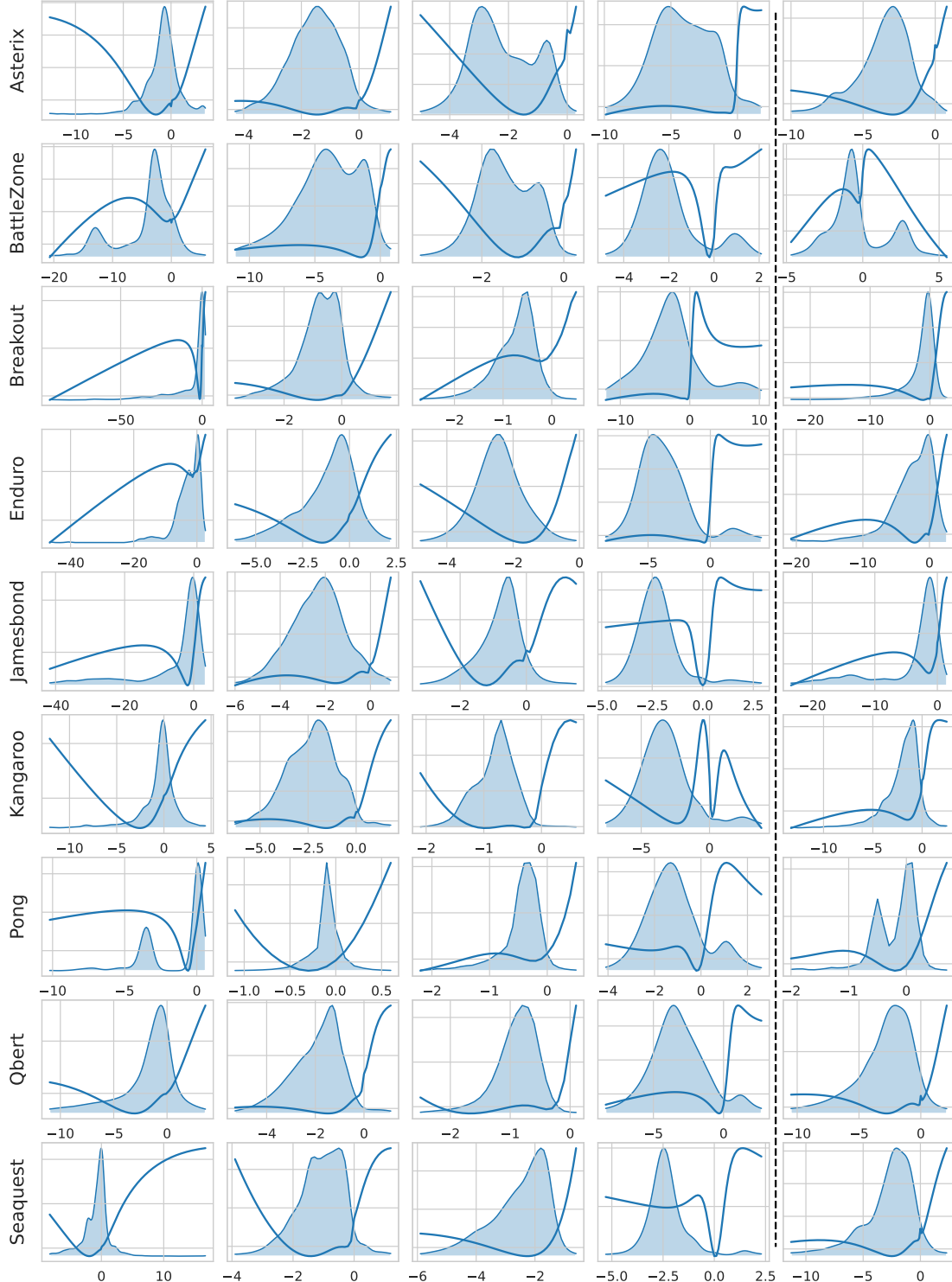


Figure 6: Images extracted from DQN agents with full plasticity playing the set of 15 Atari 2600 games used in this paper. Stationary environments (e.g. Pong, Video Pinball) do not evolve during training, dynamic ones provide different input/output distributions that are early accessible in the game (e.g Q*bert, Enduro) and progressive ones (e.g. Jamesbond, Time Pilot) require the agent to improve for the it to evolve.

A.5 Learned rational activation functions

We have explained in the main text how rational functions of agents used on different games can exhibit different complexities. This section provides the learned parametric rational functions learned by DQN agents with full plasticity (left) and by those with regularised plasticity (right) after convergence for every different tested game of the gym Atari 2600 environment. Kernel Density Estimations (with Gaussian kernels) of the input distributions indicates where the functions is most activated. Rational functions from agents of simplest games (*e.g.* Enduro, Pong, Q*bert) have simpler profiles (*i.e.* fewer distinct extrema).



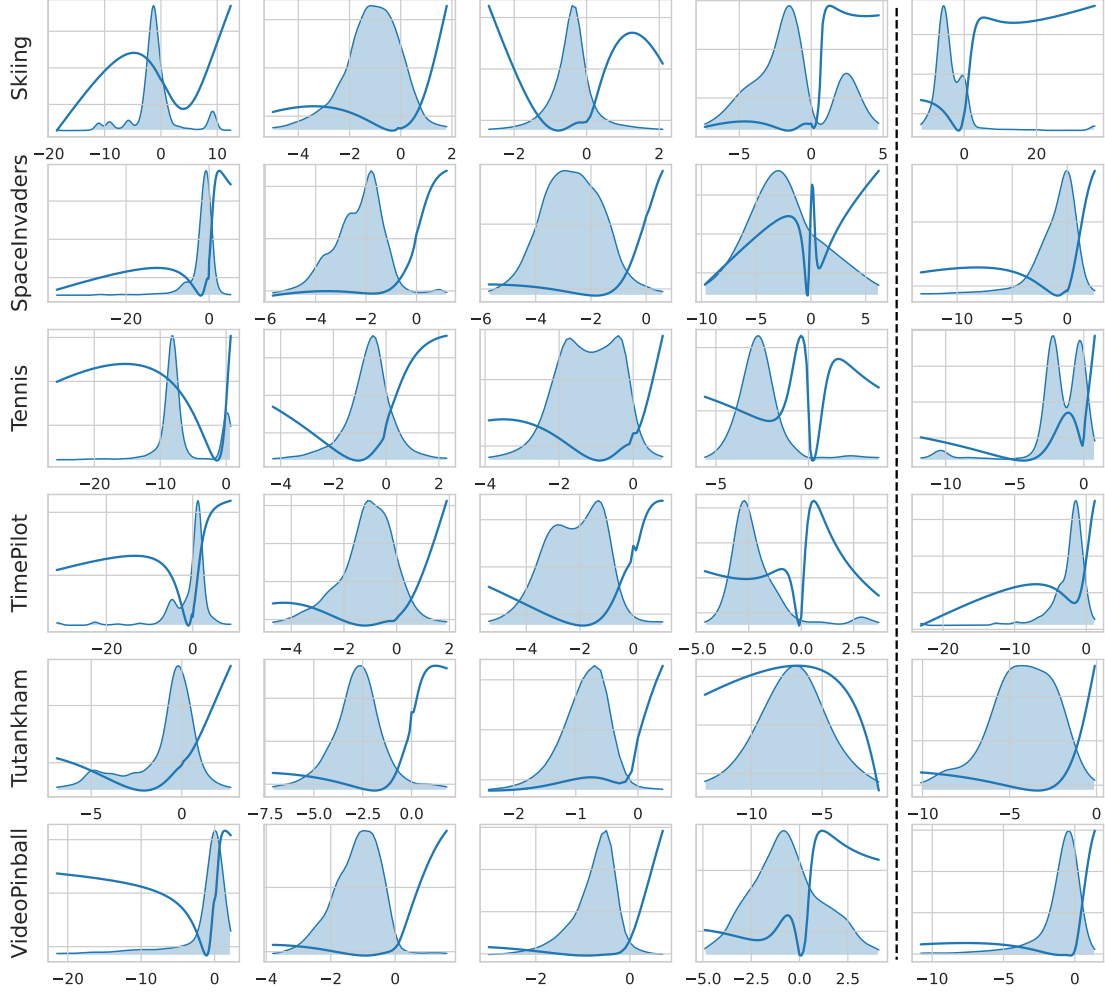


Figure 7: Profiles and input distributions of rational functions (left) and recurrent-rational ones (right) of DQN agents on the different tested games. (Recurrent-)rational functions from agents of simplest games have simpler profiles (*i.e.* fewer distinct extrema).

A.6 Technical details to reproduce the experiments

We here provide details on our experiments for reproducibility.

A.6.1 Supervised Learning Experiments

For the lesioning experiment, we used an available² pretrained Residual Network (original). We then remove the corresponding block (and potentially replace it with a identity initialised rational activation function) (surgered). We finetune the new models, allowing for optimisation of the previous and next layers (and potentially the rational function) for 15 epochs with SGD (learning rate of 0.001).

The final recovery score are computed following:

$$\text{recovery} = 100 \times \frac{\text{finetuned} - \text{surgered}}{\text{original} - \text{surgered}}, \quad (5)$$

A.6.2 Reinforcement Learning Experiments

To ease the reproducibility of our the reinforcement learning experiments, we used the *Mushroom RL* library (D’Eramo et al., 2020). We used states consisting of 4 consecutive grey-scaled images, downsampled to 84×84 .

²<https://download.pytorch.org/models/resnet101-5d3b4d8f.pth>

Network Architecture. The input to the network is thus a 84x84x4 tensor containing a rescaled, and gray-scaled, version of the last four frames. The first convolution layer convolves the input with 32 filters of size 8 (stride 4), the second layer has 64 layers of size 4 (stride 2), the final convolution layer has 64 filters of size 3 (stride 1). This is followed by a fully-connected hidden layer of 512 units.

All these layers are separated by the corresponding activation functions (either Leaky ReLU, SiLU, SiLU for convolution layers and dSiLU for linear ones, rational functions and recurrent-rational ones (of order $m = 5$ and $n = 4$, initialised to approximate Leaky ReLU).

Hyper-parameters. We evaluate the agents every 250K steps, for 125K steps. The target network is updated every 10K steps, with a replay buffer memory of initial size 500K, and maximum size 500K, except for Pong, for which all these values are divided by 10. The discount factor γ is set to 0.99 and the learning rate is 0.000025. We do not select the best policy among seeds between epochs. We use the simple ϵ -greedy exploration policy, with the ϵ decreasing linearly from 1 to 0.1 over 1M steps, and an ϵ of 0.05 is used for testing.

The only difference from the evaluation of Mnih et al. (2015) and of van Hasselt et al. (2016) evaluation is the use of the Adam optimiser instead of RMSProp, for every evaluated agent.

Normalisation techniques. To compute human normalised scores, we used the following equation:

$$\text{score}_{\text{normalised}} = 100 \times \frac{\text{score}_{\text{agent}} - \text{score}_{\text{random}}}{\text{score}_{\text{human}} - \text{score}_{\text{random}}}, \quad (6)$$

For readability, the curves plotted in the Figures 3 and 6 are smoothed following:

$$\text{score}_t = \alpha \times \text{score}_{t-1} + (1 - \alpha) \times \text{score}_t, \quad (7)$$

with $\alpha = 0.9$.